Desalination and Water Treatment
www.deswater.com
doi: 10.5004/dwt.2020.26232

203 (2020) 279–291
November

Adsorption of mercury(II) from aqueous solutions using dried *Scrophularia striata* stems: adsorption and kinetic studies

Mansooreh Dehghani[a], Majid Nozari[b], Iman Golkari[a], Nasrin Rostami[a], Marziyeh Ansari Shiri[c,*]

[a]*Department of Environmental Health, Research Center for Health Sciences, School of Health, Shiraz University of Medical Sciences, Shiraz, Iran, emails: mdehghany@sums.ac.ir (M. Dehghani), imangolkari110@gmail.com (I. Golkari), nasrinrostami676@gmail.com (N. Rostami)*
[b]*Department of Environmental Health, School of Public Health, Kerman University of Medical Sciences, Kerman, Iran, email: nozari.m@kmu.ac.ir (M. Nozari)*
[c]*Department of Environmental Health, Research Center for Health Sciences, School of Public Health, Kerman University of Medical Sciences, Kerman, Iran, Tel./Fax: +98-711-7260225; email: marziyehansari566@gmail.com (M.A. Shiri)*

Received 11 October 2019; Accepted 10 June 2020

ABSTRACT

This study aimed to assess the performance of dried *Scrophularia striata* stems (DSSS) in the removal of mercury(II) from aqueous solutions. Detailed experimental investigations were carried out to determine the effects of initial pH, adsorbent dose, initial concentration of mercury(II), and adsorption time on the adsorption capabilities of DSSS. The prepared adsorbent was characterized by Brunauer–Emmett–Teller, scanning electron microscopy, Fourier transform infrared, and energy dispersive X-ray analyses. Moreover, mercury(II) adsorption was theoretically interpreted using kinetics, isotherms, and thermodynamics models. The extent of mercury(II) adsorption was found to depend on the initial pH, adsorbent dose, initial concentration of mercury(II), and adsorption time. It was also found that the pseudo-first-order kinetic model fitted very well for mercury(II) adsorption. The Langmuir isotherm provided the best correlation for the adsorption of mercury(II). The desorption of mercury(II) by a batch process using different DSSS concentrations ranged from 96.2% to 98.7%. The results showed that DSSS could be an appropriate adsorbent for adsorption of mercury(II) from aqueous solutions.

Keywords: Adsorption; Desorption; Kinetic; Isotherm; Mercury(II); *Scrophularia striata*

1. Introduction

Mercury(II) may enter the environment and water resources through natural phenomena, such as volcanic activity and erosion of mineral deposits, or through human activities, such as mining, metallurgy, coal production, coal-fired power plants, residential heating systems, paper pulp production, incinerators, and chemical synthesis [1]. Mercury compounds turn into methylmercury in the environment, which is consumed by fish and finally by humans. Methylmercury is then distributed to human beings' central nervous system and kidneys from the gastrointestinal tract and causes cerebral palsy, seizure, hematological disorders, and cardiovascular diseases [2,3].

Various methods have been used to remove mercury(II), including biological [4], coagulation–flocculation [5], membrane technology [6], and adsorption [7,8] processes. Adsorption processes are attractive due to their

* Corresponding author.

environmental compatibility, simple design, low cost, high removal rate, ease of operation, relatively small sludge production, and adsorbent regeneration capacity [9–12].

Scrophulariaceae is a large angiosperm family, which is widely distributed in deciduous and coniferous forests of Central Europe, Central Asia, North America, and the Mediterranean area [13]. It also grows in many areas of Iran, including the Zagros Mountains in Ilam province. Given that different plants are known to be good adsorbents for the removal of heavy metals [14,15], it was hypothesized that dried *Scrophularia striata* stems (DSSS) may be a good adsorbent for this purpose. Up to now, many studies have been conducted on the removal of heavy metals via adsorption. However, no study has explored the removal of mercury(II) from aqueous solutions through adsorption using DSSS. Hence, the present study aimed to assess the removal of mercury(II) from aqueous solutions using DSSS as the adsorbent. The influence of experimental parameters, such as the initial pH, adsorbent dose, initial mercury(II) concentration, and contact time, on the adsorption process was also examined. In addition, three adsorption isotherm models, namely Langmuir, Freundlich, and Temkin, were used to determine the best-fitting model for the experimental data. The kinetic and thermodynamic parameters for the adsorption of mercury(II) using DSSS were calculated, as well.

2. Materials and methods

2.1. Adsorbent preparation

S. striata was collected from the Zagros Mountains early in the summer of 2016. Stems of the plant were separated, chopped, and washed with distilled water. Subsequently, they were placed in an oven (Model DHG-9000, Zhengzhou Protech Technology Co., Ltd., China) at 88°C for 2 h to completely dry. As a modification method, the dried stems were powdered. Then, they were washed with hydrochloric acid (10% solution) for natural dyes to be removed from the powdered stems and were rinsed with distilled water for the residual acid to be removed. Finally, the material was passed through a 60–100 mesh sieve to maintain the homogeneity of the adsorbent and reduce the variability of the adsorption data.

2.2. Adsorbate preparation

The stock solution was prepared by adding 1.35 g of $HgCl_2$ and two drops of concentrated HNO_3 (to increase acidity and prevent precipitate formation) to 200 mL distilled water. After dissolution, it was diluted to 1,000 mL with distilled water. All experiments were carried out by proper dilution of the stock solution and were conducted at ambient temperature (22°C ± 2°C) in the batch mode.

All chemicals used in this study were of analytical grade and were purchased from Merck Company (Darmstadt, Germany). The effects of contact time (20–180 min), adsorbent dosage (0.1–2 g/100 mL), initial pH (2–10), and initial concentration (2–10 mg/L) on the efficiency of mercury(II) adsorption were investigated. The adsorption equilibrium experiment for mercury(II) solution was carried out at the mercury(II) solution concentrations of 2, 3, 5, 6, 8, 9, and 10 mg/L in 250 mL Erlenmeyer flasks. The Erlenmeyer flasks were then transferred to a shaker (Model E5650 Digital Benchtop Reciprocal Shaker, Eberbach, Germany) and vibrated at 125 rpm for 24 h to ensure the equilibrium adsorption. After 24 h, the solution attained equilibrium and the amount of mercury(II) adsorbed (mg/g) on the surface of the adsorbent was determined by the difference between the two concentrations. Triplicate experiments were carried out for all variables under investigation and only the average values were taken into consideration. The contents of the flasks were filtered and analyzed for residual mercury(II) concentration. Distilled water was used as the control sample. Control samples were prepared in the same manner without using DSSS as the adsorbent. Before analysis, the samples were centrifuged at 4,500 rpm to separate the adsorbent. The residual metal concentrations were analyzed by a UV/visible spectrophotometer via 3500–HgC methods [16] using diphenylthiourea at the wavelength of 492 nm. The amount of mercury(II) adsorbed in milligram per gram was determined using the following mass balance equation [17,18]:

$$q_e = \frac{\left(C_i - C_e\right)V}{m} \tag{1}$$

Where q_e represented the amount of mercury(II) adsorbed per gram of the adsorbent (mg/g), C_i and C_e were mercury(II) concentrations (mg/L) before and after adsorption, respectively, V was the volume of adsorbate in liter, and m was the weight of the adsorbent in grams. The removal percentage of mercury(II) was calculated using the following equation:

$$\text{Removal}\left(\%\right) = \frac{\left(C_i - C_e\right)}{C_i} \times 100 \tag{2}$$

2.3. Analysis

The textural characteristics of DSSS, including specific surface area, total pore volume, and pore size distribution, were obtained from N_2 adsorption/desorption data at 77 K using a surface area analyzer with BEL sorp-mini II, Japan model. The surface area of the adsorbent was estimated by the Brunauer–Emmett–Teller (BET) equation. The total pore volume was calculated at relative pressure and p/p_0 of 0.99, and micropore volume was determined using the *t*-plot method. Mesopore volume was calculated by deducting the micropore volume from the total pore volume [19]. The porous properties of the DSSS have been presented in Table 1 and the accuracy of the values was based on the apparatus accuracy. The surface morphology of the DSSS was visualized by using scanning electron microscopy (SEM) using a Vega II Tescan, Czech model. The qualitative elemental composition of the DSSS was also determined by energy dispersive X-ray (EDX) spectroscopy using a Vega II Tescan, Czech model. The Fourier transform infrared (FTIR) spectra of the DSSS were recorded before and after mercury(II) ion adsorption in the frequency range of 400–4,000 cm^{-1} using Shimadzu, FTIR1650 spectrophotometer, Japan.

Table 1
Characteristic of DSSS

Parameter	Value
BET surface area (m^2/g)	125.14
Total pore volume (cm^3/g)	0.2123
Micropore volume (cm^3/g)	0.1206
Mesoporosity (%)	48
Average pore diameter (nm)	6.5931

2.4. Adsorption kinetics

To analyze the adsorption kinetics of mercury(II) using DSSS, pseudo-first-order, pseudo-second-order, and Elovich models were tested [12,20]. The kinetic parameters for the adsorption process were studied in a batch adsorption of 2–10 mg/L of mercury(II) at pH = 8. The adsorption time varied from 20 to 180 min and the adsorption efficiency of mercury(II) was monitored during the investigation.

2.4.1. Pseudo-first-order model

For the batch-adsorption time process where the rate of mercury(II) adsorption onto the DSSS surface was proportional to the amount of mercury(II) adsorbed from the solution phase, the pseudo-first-order kinetic equation was expressed as follows [12,20]:

$$\ln\left(q_e - q_t\right) = \ln q_e - k_1 t \tag{3}$$

where q_e and q_t represented the adsorption efficiency (mg/g) of mercury(II) at equilibrium and time t, respectively and $k_1$was the rate of the constant for pseudo-first-order adsorption (1/min).

2.4.2. Pseudo-second-order model

To describe the adsorption rate of mercury(II), the pseudo-second-order equation was expressed as follows [12,20]:

$$\frac{t}{q_t} = \frac{1}{k_2 q_e^2} + \frac{1}{q_e} t \tag{4}$$

where k_2 was the constant rate for pseudo-second-order adsorption (mg/g.min).

2.4.3. Elovich model

The Elovich or Roginsky–Zeldovich equation was expressed as follows [12,20]:

$$q_t = \beta \ln\left(\alpha\beta\right) + \beta \ln t \tag{5}$$

where α was the initial mercury(II) adsorption rate (mg/g.min) and β was the desorption constant (g/mg) during any experiment.

2.5. Adsorption isotherms

Freundlich, Temkin, and Langmuir models were examined to analyze the results of adsorption [12,20]. The correlation coefficient (R^2) was used to compare the best-fitted isotherm models. Adsorption isotherm studies were carried out with seven different initial concentrations of mercury(II) from 2 to 10 mg/L at pH = 8. In addition, the adsorption time varied from 20 to 180 min and the adsorbent dosage was 2 g/100 mL.

2.5.1. Langmuir isotherm

The Langmuir isotherm model has limited adsorption sites because of forming monolayer adsorption on the adsorbent surface. This isotherm has been presented in Eq. (6) [12,20]:

$$\frac{C_e}{q_e} = \frac{1}{K_L q_m} + \frac{C_e}{q_m} \tag{6}$$

where q_e was the amount of the adsorbate by the mass of the adsorbent (mg/g), q_m represented the adsorption efficiency, C_e was equilibrium concentration of the adsorbate (mg/L), and K_L was the Langmuir constant.

2.5.2. Freundlich isotherm

Freundlich isotherm was based on monolayer adsorption on heterogeneous adsorption sites with unequal energies. Freundlich adsorption isotherm has been described in Eq. (7) [12,20]:

$$\ln q_e = \ln k_f + \frac{1}{n} \ln C_e \tag{7}$$

where K_f (g/mg.min) and n were Freundlich constants.

2.5.3. Temkin isotherm

Temkin adsorption isotherm was calculated using Eq. (8) [12,20]:

$$q_e = B \ln A + B \ln C_e \tag{8}$$

where A and B represented the Temkin isotherm constant (L/g) and adsorption heat (J/mol), respectively.

2.6. Thermodynamic studies

The parameters of thermodynamic change in Gibb's free energy ($\Delta G°$), change in entropy ($\Delta S°$), and change in enthalpy ($\Delta H°$) for the adsorption process were determined using the following equations [21]:

$$\Delta G° = \Delta H° - T\Delta S° \tag{9}$$

$$\Delta G° = -RT \ln\left(\frac{q_e m}{C_e}\right) \tag{10}$$

Combining Eqs. (9) and (10), Eq. (11) was obtained as follows:

$$\log\left(\frac{q_e m}{C_e}\right) = \frac{\Delta S^\circ}{2.303R} + \frac{-\Delta H^\circ}{2.303RT} \quad (11)$$

where m was the adsorbent dose (g/L), q_e was the amount of mercury(II) adsorbed per unit mass of the adsorbent (mg/g), C_e was the equilibrium concentration (mg/L), T was temperature in kelvin, and q_e/C_e was the adsorption affinity.

The (ΔG°) value was calculated by knowing the enthalpy of adsorption (ΔH°) and the entropy of the adsorption (ΔS°). The values of (ΔH°) and (ΔS°) were obtained by a plot of $\ln(q_e^m/C_e)$ vs. $1/T$ using Eq. (11). When these two parameters were gained, (ΔG°) was calculated by Eq. (9).

2.7. Desorption of studies

The desorption studies were carried out by a batch process. In doing so, 50 mL of the sample containing 2 mg/L mercury(II) was treated with 2 g of the adsorbent. The pH of the solution was adjusted to 7 using 2 M HCl or 2 M NaOH. Then, it was left in contact with the adsorbent for 24 h. The solution was then filtered and the filtrate was analyzed for mercury(II). Afterwards, the adsorbent was transferred to another conical flask and treated with 50 mL of 0.05 M HCl solution. It was again filtered and the desorbed mercury(II) in the filtrate was determined. The above procedure was repeated six times.

3. Results and discussion

3.1. Surface characterization

The morphology of DSSS was studied by SEM [22] and EDX. SEM image (a_1 and b_1) and EDX spectrum (a_2 and b_2) of DSSS before (a) and after (b) mercury(II) ions adsorption have been depicted in Fig. 1. As shown in Fig. 1(a_1), DSSS had an irregular surface containing pores with different sizes and shapes. Based on Fig. 1(b_1), the surface of DSSS was in form of pores where mercury was adsorbed. By comparing the EDX spectrum of mercury(II) unloaded (a_2) and loaded (b_2) adsorbent, it could be concluded that mercury(II) was adsorbed onto the DSSS. In this work, the FTIR spectra were obtained in order to analyze the mechanism of mercury(II) adsorption and to identify the functional groups on the surface of DSSS. The FTIR spectra

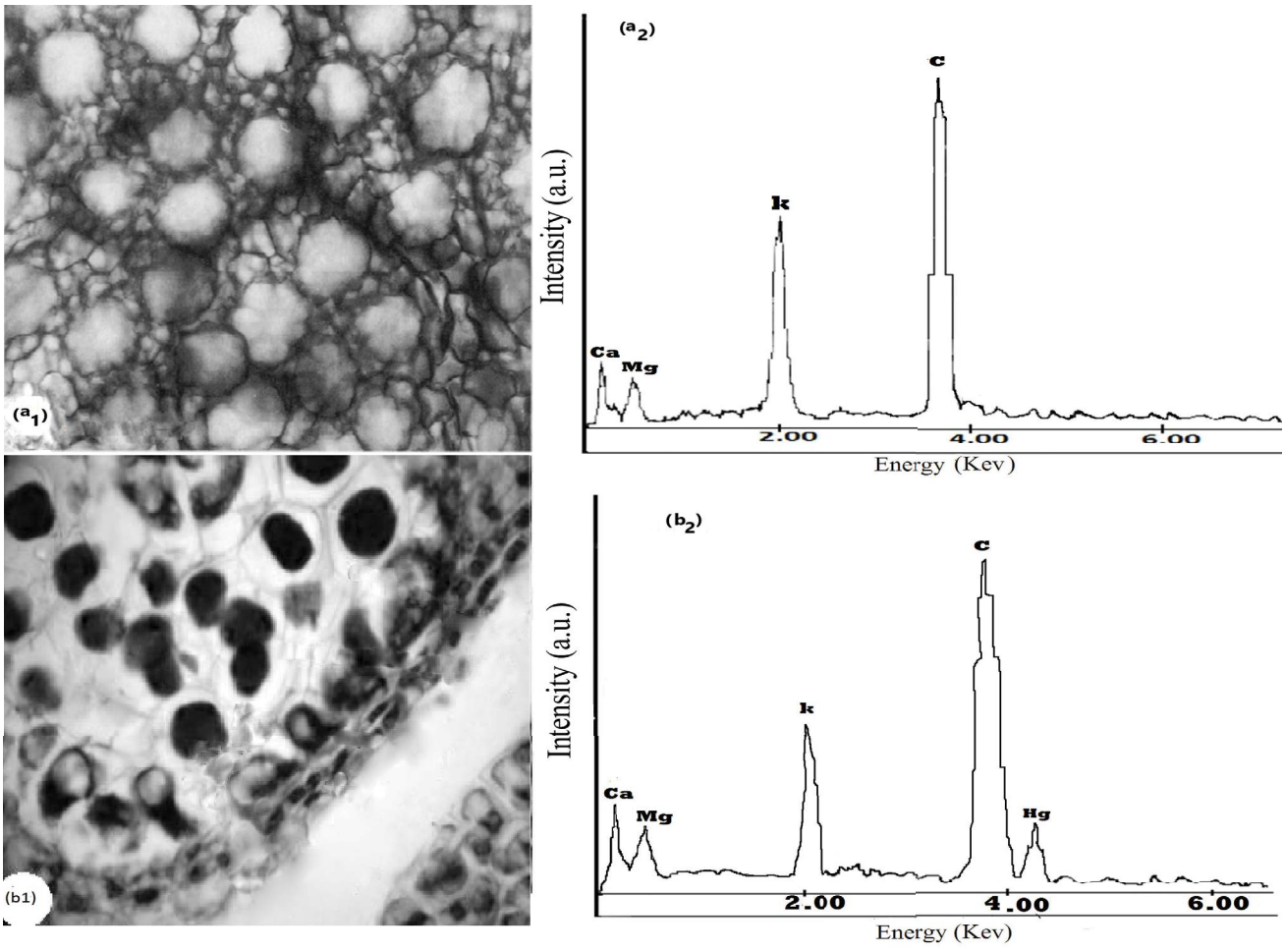

Fig. 1. SEM and EDX images of DSSS (a) before and (b) after adsorption of mercury(II).

of the adsorbent before and after mercury(II) adsorption have been presented in Fig. 2. The FTIR spectra bands indicated three major absorption bands, including carboxyl, hydroxyl, and amino groups. The differences in band intensity could be attributed to the interaction between mercury(II) ions and the functional groups on the adsorbent surface [23]. The broad absorption band at about 3,456 cm^{-1} was attributed to the complexation between –OH groups, which was shifted to 3,476 cm^{-1} after mercury(II) adsorption [18]. The next shift observed at 1,618–1,612 cm^{-1} might be due to the complexation between mercury(II) ions and carboxylic group (–C=O) [24]. According to the FTIR analysis reported in the literature [25,26], the shift observed from 1,004 to 1,031 cm^{-1} was probably due to the interaction between the nitrogen from the amino group and mercury(II). Dehghani et al. [27] used treated waste newspaper as a low-cost adsorbent. They revealed that the most abundant functional groups found on the prepared activated carbon included aromatic (C–H), carboxylic acid (C–O, C=O, and O–H), carbonyl (C=O), alkane (C–H), and amine (N–H, C–N).

3.2. Effects of the operating parameters

The solution pH affects the surface charge of the adsorbent, the degree of ionization, and the specification of the adsorbate [28,29]. The minimum and maximum adsorption efficiencies of mercury(II) were observed at pH = 2 and 8, respectively (Fig. 3a). The adsorption efficiency increased from 70% to 91% by increasing the pH from 2 to 8 and then decreased from pH = 8 to 10 (72%). The speciation models used to investigate the predominant species in the aqueous phase showed that at pH = 10, the dominant inorganic species were $Hg(OH)_2$ and OH^-. At the acidic pH, the dominant species were Hg^{2+}, H^+, and $HgOH^+$. The DSSS surface had a high positive net charge. Therefore, adsorption was not favorable for Hg^{2+}, H^+, and $HgOH^+$ cationic species. An increase in pH caused a decrease in the positive surface charge and the DSSS surface became less repulsive to cationic species, thus increasing the adsorption. At pH > 8, a decrease was detected in the adsorption of the mercury(II) species as $Hg(OH)_2$ was the predominant metal species (Fig. 4). In conclusion, at high pH levels, the dissolution of DSSS organic matter and its complexation with mercury(II) in the bulk solution seemed to be the principal factor causing the decrease in mercury(II) adsorption by DSSS. The lower adsorption efficiency in the acidic medium might be attributed to the partial protonation of the active groups and the competition of H^+ with metal ions for the adsorption sites on the DSSS. Overall, the optimal pH value of the solution for mercury(II) adsorption was 8.0. Monier [30] showed that the adsorption efficiency of mercury(II) increased by increasing the pH and that the optimum adsorption was achieved at pH = 5. Monier et al. [31] also found that a higher uptake capacity was achieved at higher pH values. In the same line, Shukla et al. [29] disclosed that the removal rate of heavy metals by the sawdust of deciduous trees could be increased by increasing the pH.

According to Fig. 3b, the adsorption efficiency of mercury(II) increased significantly by increasing the adsorbent dose up to 1 g per 100 mL, but increased slowly afterwards. The adsorption efficiency of mercury(II) for an absorbent dose of 0.1 to 2 g per 100 mL ranged from 89.2% to 93.6%. The results indicated that mercury(II) adsorption efficiency increased with an increase in the adsorbent dose. The increase in mercury(II) adsorption efficiency could be attributed to the fact that increase in the adsorbent dose caused an increase in the number of active adsorption sites and the contact surface between the adsorbent and the pollutant. In fact, by increasing the amount of the adsorbent, a large number of eligible adsorption sites would remain free. It can also be noted that considering the constant concentration of the pollutant, as the adsorbent dose increased, the ratio of active sites on the adsorbent surface area to the

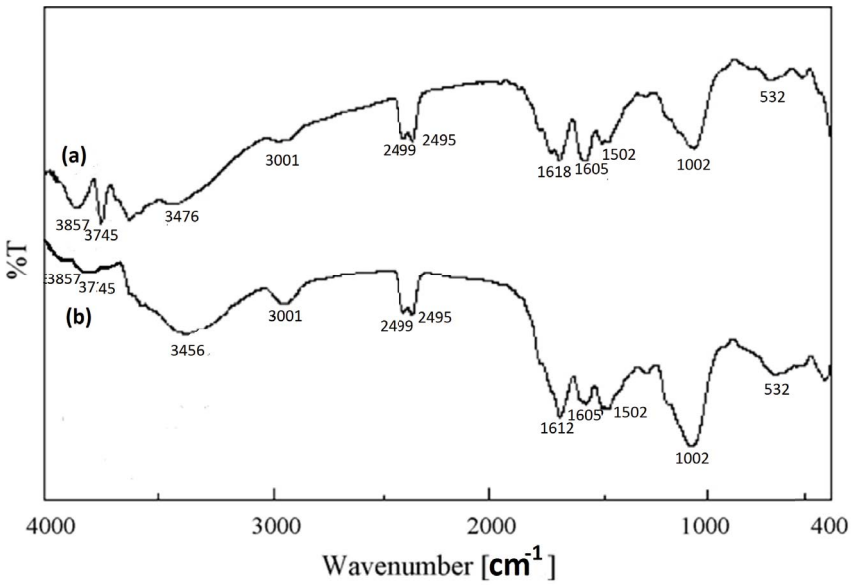

Fig. 2. FTIR spectra of the DSSS (a) without mercury(II) and (b) with mercury(II) adsorption.

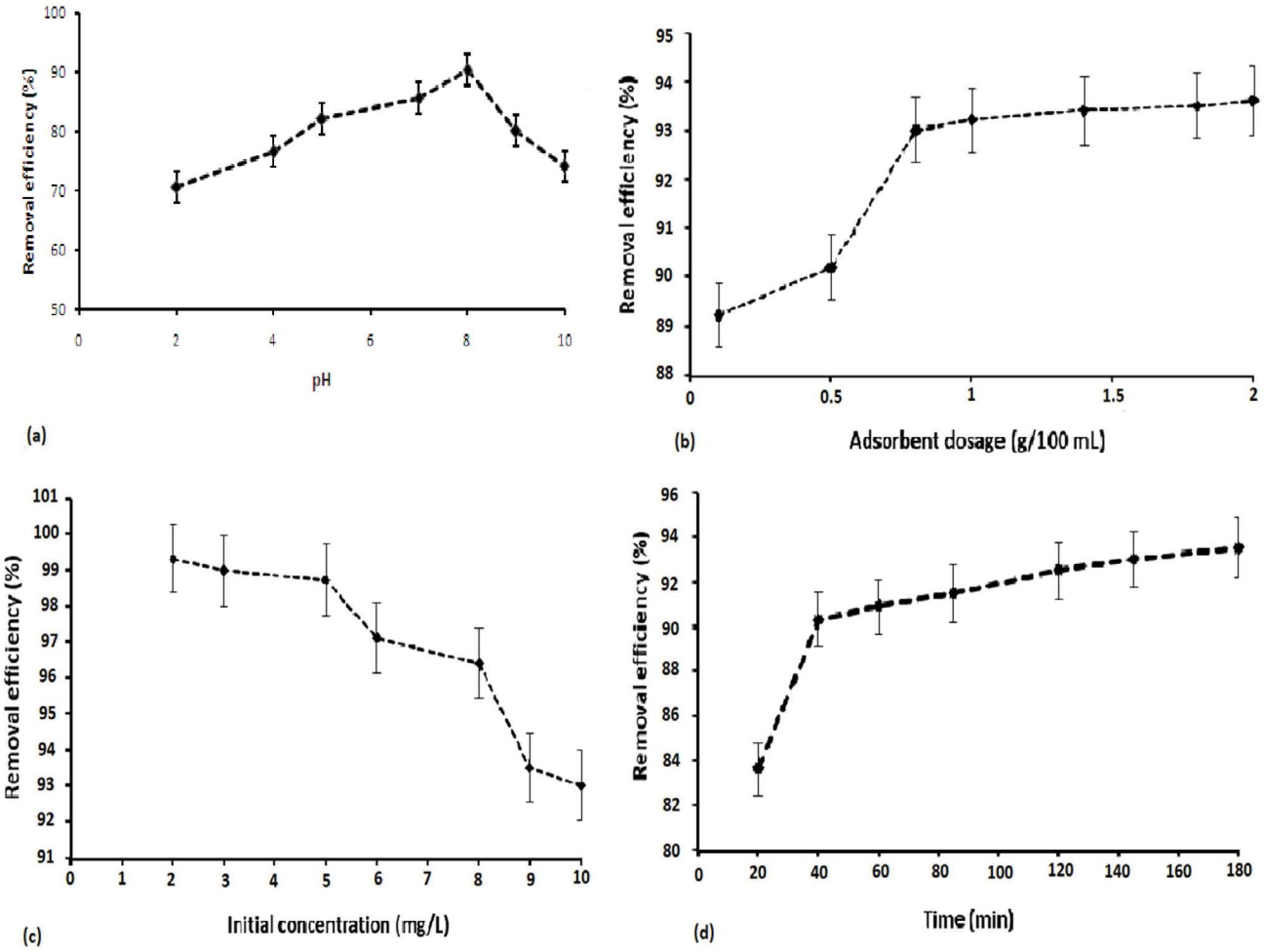

Fig. 3. (a) Adsorption efficiency of mercury(II) at different pH (the initial concentration of mercury(II):10 mg/L; adsorbent dose: 2 g/100; reaction time: 60 min), (b) adsorption efficiency of mercury(II) at different adsorbent dosage (pH = 8, the initial concentration of mercury(II): 10 mg/L, and reaction time: 60 min), (c) adsorption efficiency of mercury(II) at different initial concentrations (pH = 8, adsorbent dose: 2 g/100 mL, and reaction time: 60 min), and (d) adsorption efficiency of mercury(II) at different reaction times (pH = 8, adsorbent dose: 2 g/100 mL, and the initial concentration of mercury(II): 2 mg/L).

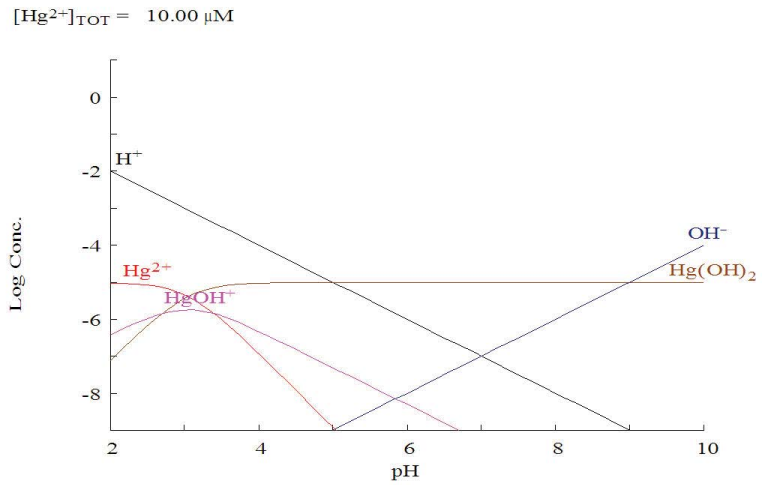

Fig. 4. Mercury(II) speciation in aqueous solution as a function of pH.

adsorbate molecules was high [12]. However, increase in the adsorbent dose could lead to the unsaturation of adsorption sites and the metal ions were inadequate to cover all the redeemable sites [32]. The optimal value of adsorbent dosage for mercury(II) adsorption was 2 g. The findings of the research by Aslam et al. [20] indicated that increase in the biomass dosage from 0.25 to 1 g increased mercury(II) adsorption. In the study conducted by Bhattacharya et al. [9], the selected adsorbents were used at the concentrations ranging from 2.5 to 30 g/L. In each case, increase in the adsorbent concentration resulted in an increase in the removal percentage of mercury(II). After a certain adsorbent dosage, however, the removal efficiency did not increase significantly.

The effect of the initial concentration of mercury(II) on the adsorption efficiency has been presented in Fig. 3c. The adsorption efficiency of mercury(II) at the initial concentrations of 2–10 mg/L ranged from 93% to 99.3%. The mercury(II) adsorption efficiency decreased with increase in the initial concentration. This could be attributed to the unavailability of free adsorption sites, limited vacancy of active sites, and increase in the ratio of mercury molecules to the surface area available for adsorption [33]. In fact, the initial concentration of mercury(II) provided a significant driving force to overcome the resistance of mass transfer between the liquid and solid phases. At low metal ion/adsorbent ratios, metal ion adsorption involved higher energy sites. As the metal ion/adsorbent ratio increased, higher energy sites were saturated and adsorption began on lower energy sites, resulting in a decrease in the adsorption efficiency [34].

The effects of reaction times (20–180 min) on the adsorption efficiency of mercury(II) were studied. As shown in Fig. 3d, the adsorption efficiency of mercury(II) increased rapidly by the increase in the adsorption time up to 40 min. A further increase in adsorption time had a negligible effect on the percentage of removal. The optimal value of the contact time for mercury(II) adsorption was 180 min. The adsorption efficiency of mercury(II) increased with the increase in the adsorption time. The nature of adsorbent and its available sorption sites affected the time needed to reach the equilibrium [9]. A study by Aslam et al. [20] found that the adsorption of mercury(II) was fast in the early stages, and the equilibrium adsorption was achieved in 40 min. Igwe et al. [35] investigated mercury(II) adsorption on unmodified and thiolated coconut fiber and indicated that with an increase in the adsorption time from 10 to 120 min, the effective adsorption of mercury(II) increased. However, a study reported the opposite results compared to those found in the present study [18].

3.3. Adsorption kinetics

The obtained experimental results were modeled using pseudo-first-order, pseudo-second-order, and Elovich kinetic models in order to describe the mechanism that controlled the adsorption of mercury(II) ion onto DSSS. The kinetic parameters of the pseudo-first-order, pseudo-second-order, and Elovich models together with the corresponding correlation coefficients (R^2) for the adsorption of mercury(II) onto DSSS at the initial mercury(II) concentrations of 2–10 mg/L have been summarized in Table 2. The correlation coefficients for the pseudo-first-order kinetic model at different concentrations ranged from 0.856 to 0.975, demonstrating a good fit in comparison to the pseudo-second-order and Elovich models. Considering the pseudo-first-order kinetic model, the plot $\ln(q_e - q_t)$ vs. t gave straight lines along the entire contact time interval (Fig. 5a). This, together with the very good correlation between the calculated and experimental values of q_e, indicated that the pseudo-first-order kinetic model was suitable for describing the kinetics of mercury(II) adsorption onto DSSS.

The pseudo-second-order kinetic model was also used to fit the experimental data (Table 2). The constant rate (K_2) and the equilibrium amount of mercury(II) ion (q_e) could be determined from the slope and intercept of the plot (Fig. 5b). The correlation coefficients for the pseudo-second-order kinetic model at different concentrations ranged from 0.846 to 0.962, indicating the limited applicability of this model in the interpretation of the experimental results. Furthermore, the values of equilibrium adsorption capacities calculated from the pseudo-second-order equation ($q_{e,\text{calc}}$, mg/g) were very different from those obtained experimentally ($q_{e,\text{exp}}$, mg/g) for all mercury(II) concenterations. Therefore, the pseudo-second-order kinetic model was not suitable for describing the kinetics of mercury(II) adsorption onto DSSS.

Considering the Elovich model (Fig. 5c), the correlation coefficients for different concentrations ranged from 0.836 to 0.954. The correlation coefficient (R^2) obtained using the Elovich kinetic model was less than those of the pseudo-first-order and pseudo-second-order kinetic models (Table 2). Therefore, the Elovich kinetic model was not suitable for describing the kinetics of mercury(II) adsorption onto DSSS.

The kinetic models for the adsorption of mercury(II) on different adsorbents, such as adulsa leaves powder, chitosan, unmodified and thiolated coconut fiber, ca-alginate and immobilized wood-rotting fungus *Funaliatrogii*, activated carbon, modified natural wool chelating fibers, live yeast *Yarrowia lipolytica* 70562, and fluorescence-sensitive adsorbent based on cellulose, have been examined by different authors [20,22,30,31,35–37]. They found that the experimental data better fitted the pseudo-second-order kinetic model.

3.4. Adsorption isotherms

In this work, different isotherm models, including the Langmuir, Freundlich, and Temkin models, were studied for mercury(II) adsorption on DSSS. The conformity of mercury(II) adsorption on DSSS had the following order based on the measured R^2 (Table 3):

Langmuir isotherm (R^2 = 0.98) > Temkin isotherm (R^2 = 0.97) > Freundlich isotherm (R^2 = 0.96).

The plot of C_e/q_e vs. C_e was analyzed to determine the Langmuir isotherm parameters, and the results have been given in Table 3. As shown in Fig. 6, the mercury(II) adsorption data were well-fitted to the Langmuir, Temkin, and Freundlich isotherms. Nonetheless, the Langmuir plot gave a better fit (Fig. 6a) to the experimental data (R^2 = 0.98). The maximum adsorption efficiency of DSSS for mercury(II) was found to be 34.24 mg/g. The values of K_f and n were determined from the plot of $\log(q_e)$ vs. $\log(C_e)$ as shown in Fig. 6b.

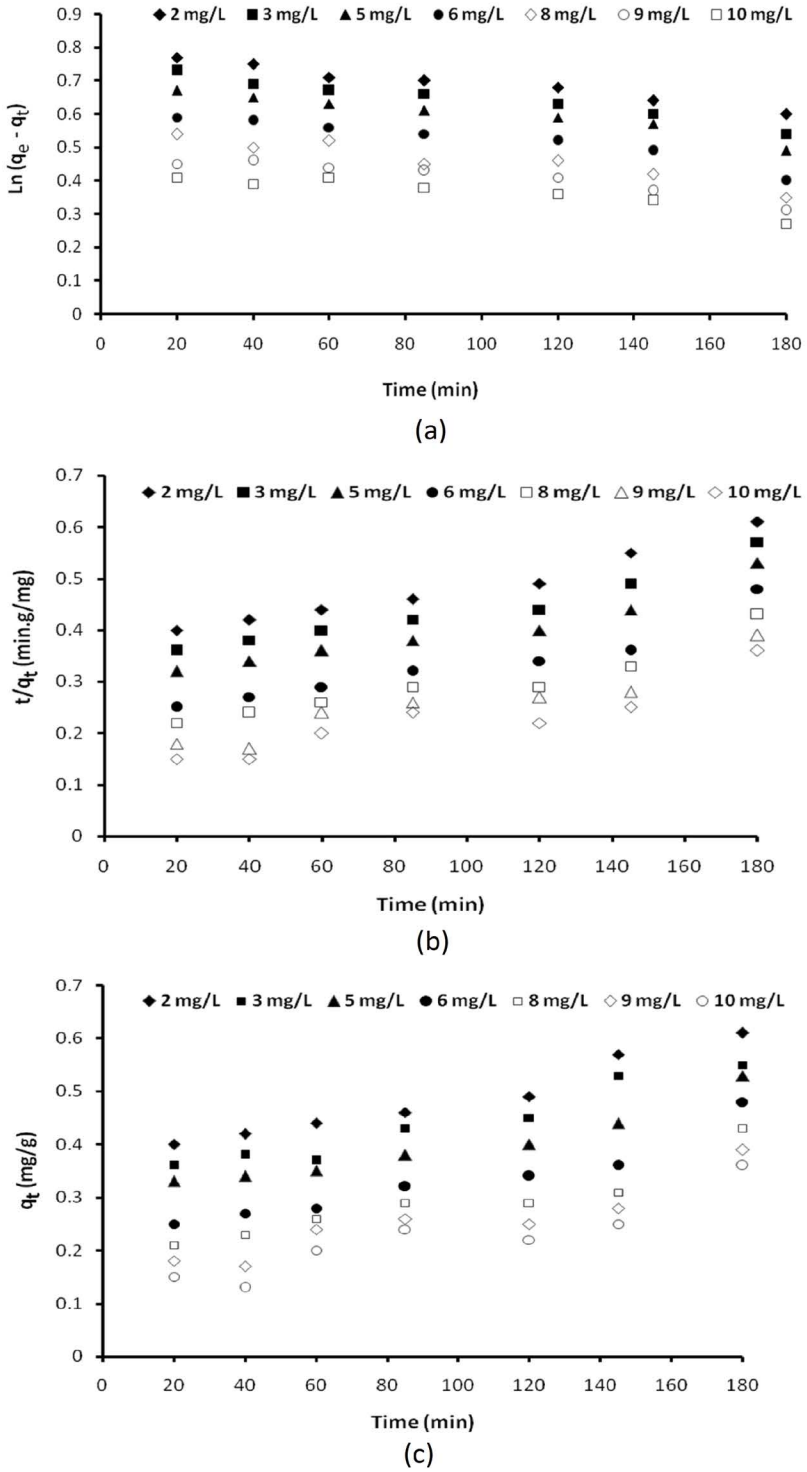

Fig. 5. Plots of adsorption first-order (a), second-order (b), and Elovich (c) kinetics, for mercury(II) on DSSS at concentrations of 2, 3, 5, 6, 8, 9, and 10 mg/L.

The K_f constant in the Freundlich equilibrium was found to be 1.39 g/L. The value of n was between 0 and 10, suggesting the relatively strong adsorption of mercury(II) onto the DSSS surface. In this study, a value of 2.186 was found for n. However, the low correlation coefficient (R^2 = 0.96) suggested that this was not the best model to describe these equilibria. Similar results for the magnitude of n have been described by several researchers [38–40].

As shown in Fig. 6c, the plot of q_e vs. lnC_e could help determine the isotherm constants A and B from the slope and

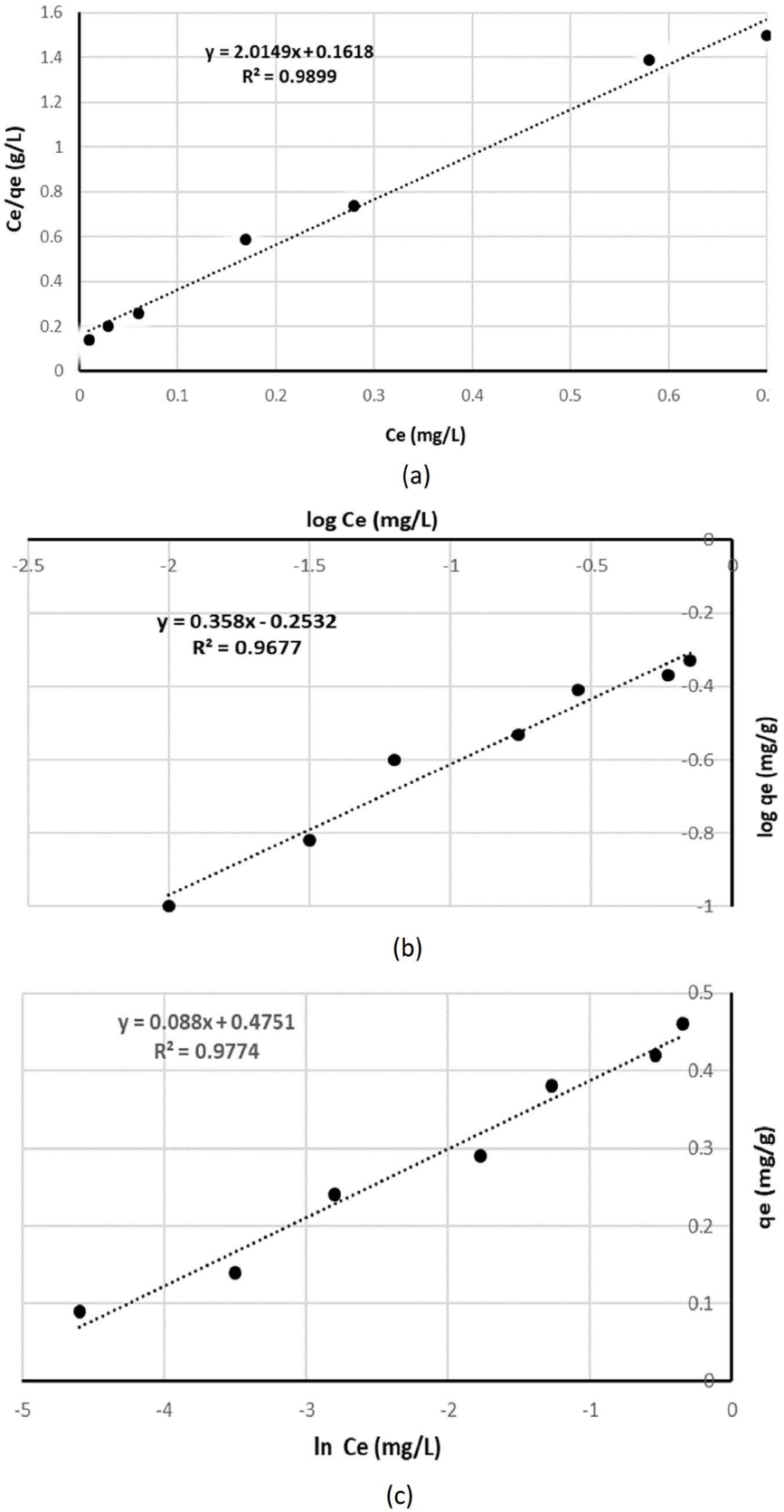

Fig. 6. Langmuir (a), Freundlich (b), and Temkin (c) isotherm models of mercury(II) onto DSSS.

Table 2
Comparison of the pseudo-first-order, pseudo-second-order, and Elovich adsorption constants for mercury(II)

Pseudo-first-order			Pseudo-second-order			Elovich			Concentration of mercury(II) (mg/L)
R^2	k_1 (×10² min⁻¹)	q_e (mg/g)	R^2	k_2 (×10² g/mg.min)	q_e (mg/g)	R^2	α	β	
0.975	4.85	29.1	0.962	10.94	35.6	0.954	0.120	32.52	2
0.966	4.68	28.5	0.936	12.45	45.7	0.933	0.188	31.81	3
0.938	4.56	27.4	0.925	13.89	52.2	0.913	0.155	31.13	5
0.912	4.43	26.5	0.896	14.52	54.5	0.887	0.112	30.24	6
0.899	4.35	25.1	0.886	15.32	63.8	0.860	0.109	29.32	8
0.887	4.26	24.9	0.873	16.25	74.6	0.840	0.106	28.64	9
0.856	4.21	24	0.846	17.54	83.4	0.836	0.105	28.50	10

Table 3
Parameters and correlation coefficient of Langmuir, Freundlich, and Temkin for mercury(II) adsorption

Langmuir model			Freundlich model			Temkin model		
K_L (L/mg)	q_m (mg/g)	R^2	K_f (g/mg.min)	N	R^2	K_T	B	R^2
0.887	35.14	0.98	1.39	2.186	0.96	0.477	12.614	0.97

intercept, respectively. The correlation coefficient (R^2 = 0.97) for the adsorption of mercury(II) in Temkin isotherm was fairly fitted well-compared to the Freundlich isotherm.

3.5. Adsorption thermodynamics

The adsorption process can be associated with the release of energy that is an exothermic process or with the absorbed energy from the surroundings that has been described as an endothermic process. The positive value of ($\Delta H°$) approved the endothermic nature of mercury(II) adsorption on DSSS, and the negative value of ($\Delta G°$) indicated the feasibility and spontaneity of the adsorption process [41].

With increase in temperature, interaction between the solvent and the solid surface might reduce the exposure of a larger number of adsorption sites. In other words, higher temperature might facilitate the adsorption of mercury(II) on the adsorbent. This could be due to the fact that increasing the temperature might produce a swelling effect within the internal structure of the adsorbent, which facilitated the penetration of mercury(II) ions into the internal structure of the adsorbent [21]. The positive value of ($\Delta S°$) showed that the adsorbed mercury(II) ions remained haphazardly over the surface of the adsorbent. The values of $\Delta H°$, $\Delta S°$, and $\Delta G°$ have been presented in Table 4. Some studies have investigated the influence of temperature on the adsorbent's structural properties, such as pore size distribution, average pore size, surface pore density, and porosity [42,43], which might be a limitation for the present study.

3.6. Adsorption mechanism

The mechanism for mercury(II) removal by adsorption on DSSS is taking place through four steps: (a) migration of mercury(II) molecules from bulk solution to the surface of the adsorbent through bulk diffusion, (b) diffusion of mercury(II) molecules through the boundary layer to the surface of the adsorbent via film diffusion; (c) the transport of the mercury(II) molecules from the surface to the interior pores of the particle occur through intra-particle diffusion or pore diffusion mechanism; and (d) the adsorption of mercury(II) at an active site on the surface of material by chemical reaction via ion-exchange, complexation, and/or chelation. In general, the mercury(II) sorption is governed by either the liquid phase mass transport rate or through the intra-particle mass transport rate [21].

Table 4
Thermodynamic parameters for adsorption of mercury(II) on DSSS

Temperature (K)	$\Delta G°$ (KJ/mol)	$\Delta S°$ (KJ/mol K)	$\Delta H°$ (KJ/mol)
298	–0.91	0.025	10.35
303	–1.3		
308	–2.06		

3.7. Desorption studies

Regeneration and reuse of DSSS is crucial for economic viability. In order to investigate the possibility of DSSS reusability, desorption, and regeneration experiments were performed and the results have been presented in Table 5. Accordingly, the desorption efficiency of mercury(II) ion using 50 mL of 0.05 M HCl solution ranged from 96.2% (cycle No. 7) to 98.7% (cycle No. 1). The desorption efficiency decreased very slowly as the number of cycles increased, but still remained high after each cycle.

Table 5
Desorption ratio of mercury(II) for various concentration of DSSS

No. of cycles	Concentration of DSSS (g/100 mL)	Desorption rate (%)
1	2	98.7
2	1.5	98
3	1.25	97. 8
4	1	97.5
5	0.75	97.2
6	0.5	97
7	0.1	96.2

Table 6
Comparison of maximum adsorption capacity of mercury(II) with various adsorbents

Adsorbents	Adsorbent efficiency (mg/g)	References
Charcoal-immobilized papain (CIP)	4.70	[44]
Camel bone charcoal	28.24	[45]
Lemna minor powder	27.62	[46]
Coconut shell	15.19	[47]
BLP	27.1	[20]
Triton X-100 modified BLP	28.1	[20]
SDS modified BLP	31.05	[20]
Eucalyptus bark	33.1	[48]
Expanded perlite	8.46	[49]
Ethylenediamine modified	30.78	[50]
Yarrowia lipolytica 70562	181.83	[37]
DSSS	35.14	[11]
DSSS	34.24	This study

3.8. Comparison to other adsorbents

The performance of the proposed method was compared to other adsorbents. Comparison of the maximum adsorption efficiency of mercury(II) ion using different types of adsorbents previously used for mercury(II) adsorption has been depicted in Table 6. Accordingly, the maximum adsorption efficiency of mercury(II) ion on DSSS was higher than that of many other previously reported adsorbents.

4. Conclusions

İn the current study, DSSS was used for adsorption of mercury(II) from an aqueous medium. The characterization of DSSS was determined using SEM, EDX, FTIR, and BET analyses. BET surface area of the prepared adsorbent was measured as 125.14 m^2/g. It was observed that the batch adsorption of mercury(II) onto DSSS depended largely on pH and that the maximum removal was achieved at pH = 8.0. DSSS was found to be an efficient adsorbent for the removal of a high amount of mercury(II) in a short time (20 min). The adsorption of mercury(II) was found to decrease with the increase in the initial mercury(II) concentration and increase with the increase in the adsorbent dosage. The equilibrium adsorption data showed a good fit to the Langmuir isotherm model and the maximum mercury(II) adsorption capacity of the adsorbent was found to be 34.24 mg/g. The pseudo-first-order model kinetic model was found to be best correlated to the experimental data for mercury(II) adsorption.

Acknowledgments

The authors would like to thank the Vice-chancellor for Research and Technology of Shiraz University of Medical Sciences for supporting the research project No. 14528. They would also like to appreciate Ms. A. Keivanshekouh at the Research Improvement Center of Shiraz University of Medical Sciences for improving the use of English in the manuscript.

Symbols

C_i — Concentration of metal ions before adsorption, mg/L
C_e — Concentration of metal ions after adsorption, mg/L
q_e — Adsorption efficiency at equilibrium status, mg/g
V — Volume of the aqueous phase, L
M — Mass of the adsorbent, g
q_t — Adsorption efficiency at t time, mg/g
q_e — Adsorption efficiency at equilibrium, mg/g
k_1 — Constant rate for the pseudo-first-order model, 1/min
k_2 — Constant rate for the pseudo-second-order model, g/mg.min
α — Initial mercury(II) concentration, mg/g min
β — Desorption constant, g/mg
q_m — Maximum adsorption efficiency, mg/g
K_L — Constant of the Langmuir isotherm, L/mg
K_f — Constant of the Freundlich isotherm, g/mg.min
n — Constant of the Freundlich isotherm
A — Constant of the Temkin isotherm, L/g
B — Heat of adsorption, J/mol
R^2 — Gas constant, kJ/mol K
T — Absolute temperature, K
$\Delta S°$ — Entropy of activation, kJ/mol K
$\Delta H°$ — Enthalpy of activation, kJ/mol
$\Delta G°$ — Free energy of activation, kJ/mol
BET — Brunauer–Emmett–Teller
EDX — Energy-dispersive X-ray
SEM — Scanning electron microscopy
FTIR — Fourier transform infrared

References

[1] X. Guo, B. Du, Q. Wei, J. Yang, L. Hu, L. Yan, W. Xu, Synthesis of amino functionalized magnetic graphenes composite material and its application to remove Cr(VI), Pb(II), Hg(II), Cd(II) and Ni (II) from contaminated water, J. Hazard. Mater., 278 (2014) 211–220.
[2] O. Hakami, Y. Zhang, C.J. Banks, Thiol-functionalised mesoporous silica-coated magnetite nanoparticles for high efficiency removal and recovery of Hg from water, Water Res., 46 (2012) 3913–3922.

[3] H. Biester, P. Schuhmacher, G. Müller, Effectiveness of mossy tin filters to remove mercury from aqueous solution by Hg(II) reduction and Hg(0) amalgamation, Water Res., 34 (2000) 2031–2036.
[4] C. Green-Ruiz, Mercury(II) removal from aqueous solutions by nonviable *Bacillus* sp. from a tropical estuary, Bioresour. Technol., 97 (2006) 1907–1911.
[5] P. Miretzky, A.F. Cirelli, Hg(II) removal from water by chitosan and chitosan derivatives: a review, J. Hazard. Mater., 167 (2009) 10–23.
[6] R. Li, L. Liu, F. Yang, Removal of aqueous Hg(II) and Cr(VI) using phytic acid doped polyaniline/cellulose acetate composite membrane, J. Hazard. Mater., 280 (2014) 20–30.
[7] M. Mureseanu, A. Reiss, N. Cioatera, I. Trandafir, V. Hulea, Mesoporous silica functionalized with 1-furoyl thiourea urea for Hg(II) adsorption from aqueous media, J. Hazard. Mater., 182 (2010) 197–203.
[8] L. Bulgariu, M. Ratoi, D. Bulgariu, M. Macoveanu, Adsorption potential of mercury(II) from aqueous solutions onto Romanian peat moss, J. Environ. Sci. Health., Part A, 44 (2009) 700–706.
[9] A. Bhattacharya, T. Naiya, S. Mandal, S. Das, Adsorption, kinetics and equilibrium studies on removal of Cr(VI) from aqueous solutions using different low-cost adsorbents, Chem. Eng. J., 137 (2008) 529–541.
[10] M. Dehghani, M.A. Shiri, S. Shahsavani, N. Shamsedini, M. Nozari, Removal of Direct Red 81 dye from aqueous solution using neutral soil containing copper, Desal. Water Treat., 86 (2017) 213–220.
[11] M. Dehghani, M. Nozari, I. Golkari, N. Rostami, M.A. Shiri, Adsorption and kinetic studies of hexavalent chromium by dehydrated *Scrophularia striata* stems from aqueous solutions, Desal. Water Treat., 125 (2018) 81–92.
[12] M. Dehghani, M. Nozari, A. Fakhraei Fard, M. Ansari Shiri, N. Shamsedini, Direct red 81 adsorption on iron filings from aqueous solutions; kinetic and isotherm studies, Environ. Technol., 40 (2019) 1705–1713.
[13] M. Rezaie-Tavirani, S.A. Mortazavi, M. Barzegar, S.H. Moghadamnia, M.B. Rezaee, Study of anti cancer property of *Scrophularia striata* extract on the human astrocytoma cell line (1321), Iran. J. Pharm. Res., 9 (2010) 403–410.
[14] A.K. Jha, U. Kumar, Studies on removal of heavy metals by *Cymbopogon flexuosus*, Int. J. Agric. Environ. Biotechnol., 10 (2017) 89–92.
[15] B.V. Tangahu, S.R. Sheikh Abdullah, H. Basri, M. Idris, N. Anuar, M. Mukhlisin, A review on heavy metals (As, Pb, and Hg) uptake by plants through phytoremediation, Int. J. Chem. Eng., 2011 (2011) 1–31.
[16] R. Zhang, B. Wang, H. Ma, Studies on chromium(VI) adsorption on sulfonated lignite, Desalination, 255 (2010) 61–66.
[17] R. Bennicelli, Z. Stępniewska, A. Banach, K. Szajnocha, J. Ostrowski, The ability of *Azolla caroliniana* to remove heavy metals (Hg(II), Cr(III), Cr(VI)) from municipal waste water, Chemosphere, 55 (2004) 141–146.
[18] N.K. Hamadi, X.D. Chen, M.M. Farid, M.G. Lu, Adsorption kinetics for the removal of chromium(VI) from aqueous solution by adsorbents derived from used tyres and sawdust, Chem. Eng. J., 84 (2001) 95–105.
[19] F. Gorzin, A.A. Ghoreyshi, Synthesis of a new low-cost activated carbon from activated sludge for the removal of Cr(VI) from aqueous solution: equilibrium, kinetics, thermodynamics and desorption studies, Korean J. Chem. Eng., 30 (2013) 1594–1602.
[20] M. Aslam, S. Rais, M. Alam, A. Pugazhendi, Adsorption of Hg(II) from aqueous solution using Adulsa (*Justicia adhatoda*) leaves powder: kinetic and equilibrium studies, J. Chem., 2013 (2013) 1–11.
[21] D.K. Mondal, B.K. Nandi, M. Purkait, Removal of mercury(II) from aqueous solution using bamboo leaf powder: equilibrium, thermodynamic and kinetic studies, J. Environ. Chem. Eng., 1 (2013) 891–898.
[22] M.Y. Arıca, G. Bayramoğlu, M. Yılmaz, S. Bektaş, Ö. Genç, Biosorption of Hg^{2+}, Cd^{2+}, and Zn^{2+} by Ca-alginate and immobilized wood-rotting fungus *Funalia trogii*, J. Hazard. Mater., 109 (2004) 191–199.
[23] G. Sharma, D. Pathania, M. Naushad, Preparation, characterization, and ion exchange behavior of nanocomposite polyaniline zirconium(IV) seleno tungstophosphate for the separation of toxic metal ions, Ionics, 21 (2015) 1045–1055.
[24] L. Levankumar, V. Muthukumaran, M. Gobinath, Batch adsorption and kinetics of chromium(VI) removal from aqueous solutions by *Ocimum americanum* L. seed pods, J. Hazard. Mater., 161 (2009) 709–713.
[25] M. Bansal, D. Singh, V. Garg, A comparative study for the removal of hexavalent chromium from aqueous solution by agriculture wastes' carbons, J. Hazard. Mater., 171 (2009) 83–92.
[26] A.K. Giri, R. Patel, S. Mandal, Removal of Cr(VI) from aqueous solution by *Eichhornia crassipes* root biomass-derived activated carbon, Chem. Eng. J., 185 (2012) 71–81.
[27] M.H. Dehghani, D. Sanaei, I. Ali, A. Bhatnagar, Removal of chromium(VI) from aqueous solution using treated waste newspaper as a low-cost adsorbent: kinetic modeling and isotherm studies, J. Mol. Liq., 215 (2016) 671–679.
[28] M. Dehghani, S. Nasseri, M. Karamimanesh, Removal of 2,4-dichlorophenolyxacetic acid (2,4-D) herbicide in the aqueous phase using modified granular activated carbon, J. Environ. Health. Sci. Eng., 12 (2014) 28.
[29] A. Shukla, Y.-H. Zhang, P. Dubey, J. Margrave, S.S. Shukla, The role of sawdust in the removal of unwanted materials from water, J. Hazard. Mater., 95 (2002) 137–152.
[30] M. Monier, Adsorption of Hg^{2+}, Cu^{2+} and Zn^{2+} ions from aqueous solution using formaldehyde cross-linked modified chitosan–thioglyceraldehyde Schiff's base, Int. J. Biol. Macromol., 50 (2012) 773–781.
[31] M. Monier, D. Ayad, A. Sarhan, Adsorption of Cu(II), Hg(II), and Ni(II) ions by modified natural wool chelating fibers, J. Hazard. Mater., 176 (2010) 348–355.
[32] N. Saifuddin, A. Raziah, Removal of heavy metals from industrial effluent using *Saccharomyces cerevisiae* (Baker's yeast) immobilized in chitosan/lignosulphonate matrix, J. Appl. Sci. Res., 3 (2007) 2091–2099.
[33] P. Mokhtari, M. Ghaedi, K. Dashtian, M. Rahimi, M. Purkait, Removal of methyl orange by copper sulfide nanoparticles loaded activated carbon: kinetic and isotherm investigation, J. Mol. Liq., 219 (2016) 299–305.
[34] A.I. Zouboulis, N.K. Lazaridis, K.A. Matis, Removal of toxic metal ions from aqueous systems by biosorptive flotation, J. Chem. Technol. Biotechnol., 77 (2002) 958–964.
[35] J.C. Igwe, A. Abia, C. Ibeh, Adsorption kinetics and intraparticulate diffusivities of Hg, As and Pb ions on unmodified and thiolated coconut fiber, Int. J. Environ. Sci. Technol., 5 (2008) 83–92.
[36] M. Li, B. Li, L. Zhou, Y. Zhang, Q. Cao, R. Wang, H. Xiao, Fluorescence-sensitive adsorbent based on cellulose using for mercury detection and removal from aqueous solution with selective "on-off" response, Int. J. Biol. Macromol., 132 (2019) 1185–1192.
[37] E.A. Dil, M. Ghaedi, G.R. Ghezelbash, A. Asfaram, M.K. Purkait, Highly efficient simultaneous biosorption of Hg^{2+}, Pb^{2+} and Cu^{2+} by Live yeast *Yarrowia lipolytica* 70562 following response surface methodology optimization: kinetic and isotherm study, J. Ind. Eng. Chem., 48 (2017) 162–172.
[38] Y.-M. Hao, C. Man, Z.-B. Hu, Effective removal of Cu(II) ions from aqueous solution by amino-functionalized magnetic nanoparticles, J. Hazard. Mater., 184 (2010) 392–399.
[39] T.K. Naiya, A.K. Bhattacharya, S.K. Das, Adsorption of Cd(II) and Pb(II) from aqueous solutions on activated alumina, J. Colloids Interface Sci., 333 (2009) 14–26.
[40] J. Hu, G. Chen, I.M. Lo, Removal and recovery of Cr(VI) from wastewater by maghemite nanoparticles, Water Res., 39 (2005) 4528–4536.
[41] M. Ghaedi, A. Shokrollahi, H. Tavallali, F. Shojaiepoor, B. Keshavarz, H. Hossainian, M. Soylak, M.K. Purkait, Activated carbon and multiwalled carbon nanotubes as efficient adsorbents for removal of arsenazo(III) and methyl red from waste water, Toxicol. Environ. Chem., 93 (2011) 438–449.
[42] C. Lattao, X. Cao, J. Mao, K. Schmidt-Rohr, J.J. Pignatello, Influence of molecular structure and adsorbent properties on

sorption of organic compounds to a temperature series of wood chars, Environ. Sci. Technol., 48 (2014) 4790–4798.
[43] D. Ghosh, M. Sinha, M. Purkait, A comparative analysis of low-cost ceramic membrane preparation for effective fluoride removal using hybrid technique, Desalination, 327 (2013) 2–13.
[44] S. Dutta, A. Bhattacharyya, P. De, P. Ray, S. Basu, Removal of mercury from its aqueous solution using charcoal-immobilized papain (CIP), J. Hazard. Mater., 172 (2009) 888–896.
[45] S.S. Hassan, N.S. Awwad, A.H. Aboterika, Removal of mercury(II) from wastewater using camel bone charcoal, J. Hazard. Mater., 154 (2008) 992–997.
[46] S.-X. Li, F.-Y. Zheng, Y. Huang, J.-C. Ni, Thorough removal of inorganic and organic mercury from aqueous solutions by adsorption on *Lemna minor* powder, J. Hazard. Mater., 186 (2011) 423–429.
[47] J. Goel, K. Kadirvelu, C. Rajagopal, Competitive sorption of Cu(II), Pb(II) and Hg(II) ions from aqueous solution using coconut shell-based activated carbon, Adsorpt. Sci. Technol., 22 (2004) 257–273.
[48] I. Ghodbane, O. Hamdaoui, Removal of mercury(II) from aqueous media using *eucalyptus* bark: kinetic and equilibrium studies, J. Hazard. Mater., 160 (2008) 301–309.
[49] H. Ghassabzadeh, A. Mohadespour, M. Torab-Mostaedi, P. Zaheri, M.G. Maragheh, H. Taheri, Adsorption of Ag, Cu and Hg from aqueous solutions using expanded perlite, J. Hazard. Mater., 177 (2010) 950–955.
[50] Y. Liu, X. Sun, B. Li, Adsorption of Hg^{2+} and Cd^{2+} by ethylenediamine modified peanut shells, Carbohydr. Polym., 81 (2010) 335–339.